

GaP-filled PCF with ultra-high birefringence and nonlinearity for distinctive optical applications

N. Mohammadd^a, L. F. Abdulrazak^b, S. R. Tahhan^c, R. Amin^a, S. M. Ibrahim^d,
K. Ahmed^{e,f,*}, F. M. Bui^c

^a*Dept. of Electrical and Electronic Engineering, Ahsanullah University of Science and Technology, Dhaka-1208, Bangladesh*

^b*Department of Computer Science, Cihan University Sulaimaniya, Sulaimaniya 46001, Kurdistan Region, Iraq*

^c*Department of Laser and Optoelectronic Engineering, Al-Nahrain University, Baghdad, Iraq*

^d*Department of Biochemistry, College of Science, King Saud University, P.O. Box: 2455, Riyadh 11451, Saudi Arabia*

^e*Department of Electrical and Computer Engineering, University of Saskatchewan, 57 Campus Drive, Saskatoon, SK S7N 5A9, Canada*

^f*Group of Bio-photomatiç, Department of Information and Communication Technology, Mawlana Bhashani Science and Technology University, Santosh, Tangail-1902, Bangladesh*

A gallium phosphide (GaP) based photonic crystal fiber (PCF) with hexagonal air hole arrangements is introduced in this study that reveals high birefringence (Br) and nonlinear coefficient (NLC). Numerous optical properties, such as birefringence, nonlinearity, dispersion, confinement loss, effective area, core power fraction, etc. are studied by fine-tuning the geometrical variables, applying the finite element method (FEM). The numerical analyses demonstrate that an ultra-high Br of 59.1×10^{-2} and NLC of $2.37 \times 10^5 \text{ W}^{-1} \text{ Km}^{-1}$ with a large negative dispersion of $-3875.21 \text{ ps. nm}^{-1} \cdot \text{km}^{-1}$ can be accomplished at the wavelength of $1.55 \mu\text{m}$. Consequently, the developed PCF can be applied in a plethora of intriguing applications, including supercontinuum generation, telecommunications, etc.

(Received December 21, 2021; Accepted March 6, 2022)

Keywords: Photonic crystal fiber, Nonlinearity, Birefringence, Negative dispersion, Power fraction

1. Introduction

A photonic crystal is a low-loss cyclical dielectric medium made up of an adequate cyclic array of tiny air-holes that travels the length of the fiber. Photonic crystal fibers (PCFs) are a unique and advance type of optical fibers that are based upon the optical characteristics of photonic crystals. They were initially introduced by Russell et al. [1–5] and are one of the most widely used optical fibers today. A new genre of optical waveguides has been established employing PCFs capable of guiding an electromagnetic field (EMF) through an anisotropic form of material [6]. It is worth noting that the core and cladding precincts of such advanced fibers are formed employing a photonic crystal and eventually, light will transmit through the core region using the notion of total internal reflection (TIR) since the core region has a higher RI than the cladding region. The traditional optical fibers possess rigid design constraints, such as restricted core size and material choices [7–9], resulting in light propagation over a small distance. However, in PCFs, maximal light propagation occurs in the core area, which needs a higher RI than the cladding area and this is achieved by constructing the clad via micro-structured air holes [10–11].

*Corresponding author: kawsar.ict@mbstu.ac.bd
<https://doi.org/10.15251/JOR.2022.182.129>

Researchers and engineers have been influenced by the design freedom and tremendous optical characteristics of PCF that are suitable for a wide range of applications, resulting in improvements to the shortcomings of the traditional fibers. In light of this, a handsome number of unique designs have been introduced in order to actualize their distinctive qualities in diverse sectors of optics and photonics. Optical features, including ultra-high birefringence [12–13] and nonlinearity [14], flexible chromatic dispersion [15], supercontinuum generation [16], indefinite single-mode operation [17] and so on can be controlled by modifying structural forms and geometry, giving significantly improved control over the mentioned factors. Furthermore, as compared to the traditional fibers, PCF offers a wide range of adjustable qualities in core and cladding regions, as well as in pitch, backdrop material and air hole diameter, etc. These special traits are only achievable with PCF, although they would be impossible in regular optical fibers. Among the above-mentioned features, the most important attributes of PCF are ultra-high birefringence and nonlinearity. High birefringence offers a great number of intriguing uses, including retaining polarization and fiber optic sensor arrangement [18]. There are several other prominent aspects of high nonlinearity as well, including optical switching, non-linear optics, supercontinuum generation, extraordinary power transmission, laser utilization [19], etc.

Nowadays, new articles are being proposed to enhance the optical characteristics of PCF and the number of such articles is growing. In light of this, Paul et al. stated a Si_7N_3 filled rectangular PCF that displays a maximum nonlinearity of $48850 W^{-1}Km^{-1}$ at $1 \mu m$ wavelength [19]. Besides, Yang et al. stated a silica-based PCF that can achieve maximum birefringence and nonlinearity up to the order of 10^{-2} and $68 W^{-1}Km^{-1}$ respectively at the functioning wavelength of $1.55 \mu m$ [20]. In another study, Yu et al. suggested a flattened hexagonal structured PCF with a maximum birefringence and nonlinearity of 1.59×10^{-2} and $52.80 W^{-1}Km^{-1}$ respectively at $1.55 \mu m$ wavelength, where silica is used as the backdrop substance [21]. Also, Hossain et al. reported a chalcogenide glass-based PCF where the circular air holes are arranged in a mere square lattice form. Their designed PCF can obtain birefringence and nonlinearity as high as 29.78×10^{-2} and $6585 W^{-1}Km^{-1}$, sequentially [22]. Another group of researchers, Hui et al., submitted a chalcogenide-based hexagonal lattice PCF with dual-rhombic air holes that can accomplish large birefringence and nonlinearity of 4.1×10^{-2} and $4375 W^{-1}Km^{-1}$, sequentially [23]. Moreover, Zhanqiang et al. came up with a chalcogenide-based PCF, composed of a focal defect core that is enclosed by two distinct types of elliptical air holes that are each of a different size. Their investigated structures can attain birefringence and nonlinearity as high as 11.76×10^{-2} and $49760 W^{-1}Km^{-1}$, respectively [24]. In another study, Wang et al. reported a tellurite glass-filled PCF, where the cladding and core air holes are systematized in hexagonal and rectangular structures, sequentially. Their designed PCF is capable of obtaining maximum birefringence and nonlinearity of 5.05×10^{-2} and $1896 W^{-1}Km^{-1}$, sequentially [25]. Consequently, Liu et al. offered a tellurite glass-based PCF that can achieve large birefringence and nonlinearity of 7.57×10^{-2} and $188.39 W^{-1}Km^{-1}$ sequentially, at $1.55 \mu m$ wavelength [26]. Besides, Ahmed et al. stated a D-shaped PCF where the elliptical core is filled with graphene, as well as silica is employed as the background material. It is worth noting that both of these materials have different melting temperatures, making the fabrication process relatively complex and strenuous [27]. Moreover, Anas et al. purposed a GaP-based PCF that manifests high nonlinearity and birefringence of $9.47 \times 10^4 W^{-1}Km^{-1}$ and 25.9×10^{-2} respectively, at $1.4 \mu m$ wavelength [28]. However, they also used dual-material in their modeled PCF, where both materials consist of distinctive melting temperatures, making the structure very complicated and it will be quite challenging to fabricate such a tough design. In another article, Paul et al. introduced a circular-shaped hybrid PCF that displays a high nonlinearity of $63435.74 W^{-1}Km^{-1}$ at $1.00 \mu m$ wavelength [29]. The authors did not discuss various important optical properties, such as birefringence, confinement loss and so on in their manuscript. They also employed two different materials with two distinctive melting temperatures, which is another major setback of their research study. Hassan et al. reported a D-shaped PCF, where they employed silica as the background material and the core of the design is filled with As_2S_3 and As_2S_5 . Their modeled PCF obtain birefringence and nonlinearity as high as 25.4×10^{-2} and $9.114 \times 10^4 W^{-1}Km^{-1}$, sequentially [30]. They also applied dual material in a sole PCF where both the materials are of

separate melting temperatures. Moreover, due to their D-shaped structure, the polishing technique will be required even if they manage to fabricate such a complex structure, which is quite challenging in practice.

Consequently, Ahmed et al. offered a BK7 and ZBLAN filled PCF, where various optical guiding traits are investigated between the wavelength range of 1.2 to $2 \mu\text{m}$ [31]. The aforementioned literature shows that a decent number of background materials have been utilized to adjust the guiding characteristics of PCF, including silica [20–21, 32–35], ZBLAN [31], chalcogenide [23–24], tellurite [38, 56], graphene [31], GaP [44], As_2S_3 [36–37], Si_7N_3 [19], GaAs [39–41], TOPAS [54–55] and so on. Silica is the most often utilized background material among the materials listed above. Nevertheless, it can only achieve low Br and minimal NLC when used in this regard. As a result, taking the major setbacks of silica into account, various additional substances are regularly employed in order to acquire greater Br and higher NLC outcomes. GaP is the second most popular background material due to the numerous unique and remarkable qualities it possesses. The high refractive index (RI) trait of GaP plays a notable role in obtaining exceptionally high birefringence and nonlinearity. Furthermore, it should be noted that GaP has recently gained immense popularity as a non-linear optical frequency mixing substance for quasi-phase-matching (QPM) approaches, thanks to a decent number of appealing and distinctive features, namely broad transparency continuing to the spectrum of visible wavelength, extremely huge thermal conductivity, as well as it exhibits relatively minimal linear and nonlinear absorption at a wide range of wavelength spectra [42]. As a result, GaP is considered the most appropriate choice for applications requiring high Br and NLC properties.

We propose a novel GaP-based PCF with hexagonal air hole arrangements in the clad that yields remarkably ultra-high Br and NLC of 59.1×10^{-2} and $2.37 \times 10^5 \text{ W}^{-1}\text{Km}^{-1}$ sequentially, at the operating wavelength of $1.55 \mu\text{m}$. Our simulated and obtained outcomes, to the best of our knowledge, are far superior to all the formerly reported investigations in this specified research field. GaP is used as the background material in this research study due to the many advantages it possesses over other existing materials. For instance, the high RI feature of GaP is very influential in reaching particularly ultra-high birefringence and nonlinearity. Moreover, we have rigorously addressed and explored the diverse relevant distinguished optical properties of GaP-filled PCF, among which, birefringence, nonlinearity, core power fraction (CPF), confinement loss (CL), effective area, dispersion, etc. are note-worthy. Furthermore, we have discussed numerous conventional and advanced fabrication techniques in our research paper. Conclusively, our modeled PCF design can play a critical role in numerous fields of optics and photonics, namely supercontinuum generation, telecommunications, biomedical imaging and signal processing, extremely high nonlinear utilization, etc.

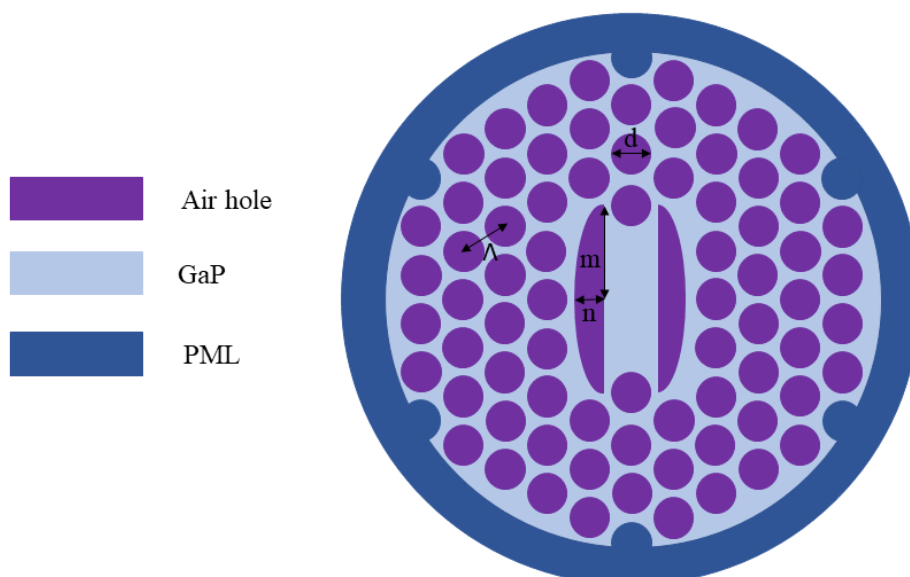


Fig. 1. Schematic diagram of the modeled GaP-based hexagonal-timbered PCF.

2. Modelling

The FEM-based COMSOL software is applied to perform an out-and-out investigation on the guiding features of our propounded PCF adopting the circular perfectly matched layer (PML) condition. Our proposed design is of hexagonal structure, where 5 rings are used and 6 air holes are deliberately omitted from the fifth ring, as illustrated in Fig. 1. The space between two neighboring air holes is designated as the pitch (Λ) in our design and the value of Λ is calculated to be $0.2 \mu\text{m}$. Besides, a few air holes are omitted from the first and second rings of the core design and placed in half ellipses on either side of the X-axis, whose major and minor semi-axes are sequentially supposed to be m and n , where $m = 1.95 \times \Lambda$ and $n = 0.65 \times \Lambda$, as well as the diameter of the circular fashioned air holes, $d = 0.9 \times \Lambda$. It is worth addressing that the pitch is the only self-reliant variable in our design on which the other parameters, such as d , m , n , etc. are entirely dependent. Moreover, we have employed GaP as the background material in our design owing to the high RI quality of it, which assists in gaining extremely high Br and NLC. Furthermore, it should be stated that we have taken a 10% thickness of PML of the total PCF.

3. Equational analyses

Analyses of the RI of GaP at room temperature have been detailed in Ref. [43], as well as required measurements have been carried out across a broad wavelength spectrum covering the visible to microwave wavelength range. A Sellmeier expression consisting of several poles for GaP has been displayed employing the frequency-dependent formula for the dielectric constant, as derived in Ref. [43]. The expression is as follows [44]:

$$n(\lambda) = \sqrt{1 + \frac{P_1\lambda^2}{\lambda^2 - Q_1} + \frac{P_2\lambda^2}{\lambda^2 - Q_2} + \frac{P_3\lambda^2}{\lambda^2 - Q_3}} \quad (1)$$

where P_1 , P_2 , P_3 and Q_1 , Q_2 , Q_3 are sellmeier constants whose values are obtained from [44]. Birefringence (Br) is defined as the contrast of effective RI between the two polarized modes (X and Y), which can be computed as follows [41]:

$$Br = |n_x - n_y| \quad (2)$$

Effective mode area is an important parameter for optical fibers. It is defined as the proportion of overall energy density per unit length of a mode to its peak energy density and it is indicated as A_{eff} . It is worth noting that when it comes to nonlinear effects, the smaller modal effective area is the most appropriate, while laser and communication devices benefit from a greater modal effective area. It can be computed from the subsequent expression [45]:

$$A_{eff} = \frac{(\iint E^2 dx dy)^2}{\iint E^4 dx dy} \quad (3)$$

where E represents the electric field of various modes. Nonlinearity is another leading aspect that needs to be assessed. The high density of power required for non-linear effects to be meaningful is provided by a minimal effective area. Nonlinearity is normally only seen at very high light intensities, which is unusual. However, PCFs are projected to have significant nonlinearity since they can restrict high-intensity light. It can be estimated from the subsequent equation [46, 53]:

$$\gamma = \frac{2\pi}{\lambda} \times \frac{n_2}{A_{eff}} W^{-1} Km^{-1} \quad (4)$$

Here, n_2 expresses the non-linear RI of GaP and its value is obtained from Ref. [47]. Another crucial feature of PCFs is dispersion, which is represented by the symbol $D(\lambda)$. Dispersion is essential in data transmission since it allows faster data transfer. Using the FEM technique, it is feasible to assess the optimum RI from the maxwell equation, as illustrated below [48]:

$$D(\lambda) = -\frac{\lambda}{c} \times \frac{d^2 Re[n_{eff}]}{d\lambda^2} \text{ ps. nm}^{-1} \cdot \text{km}^{-1} \quad (5)$$

Here, $Re(n_{eff})$, λ and c indicate the real portion of RI, operating wavelength and light velocity in a vacuum, sequentially. Power fraction is another leading trait of optical fibers that can be computed from the subsequent expression [38]:

$$\text{Core power fraction} = \frac{\int_i^n S_z dA}{\int_{total}^n S_z dA} \times 100\% \quad (6)$$

Here, 'i' denotes the core and cladding region, whereas S_z expresses the time-averaged Poynting vector. Confinement losses, symbolized as CL , are the types of losses that are largely caused by the leaky character of the modes. These types of losses can be assessed through the imaginary portion of the propagation constant, as illustrated in [49, 56]:

$$CL = 8.868 \times k_0 \times I_m[n_{eff}] \times 10^4 \text{ [dB/cm]} \quad (7)$$

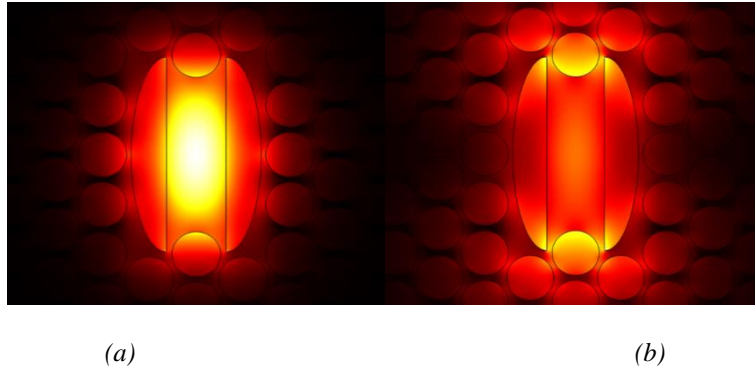


Fig. 2. Mode field distribution of (a) major and (b) minor fundamental modes at the wavelength of 1.55 μm .

4. Simulated results explorations

A special remark should be made of the fact that Figs. 2(a) and 2(b) represent the polarization of major and minor fundamental modes, respectively, which are comprehensively explored by COMSOL software.

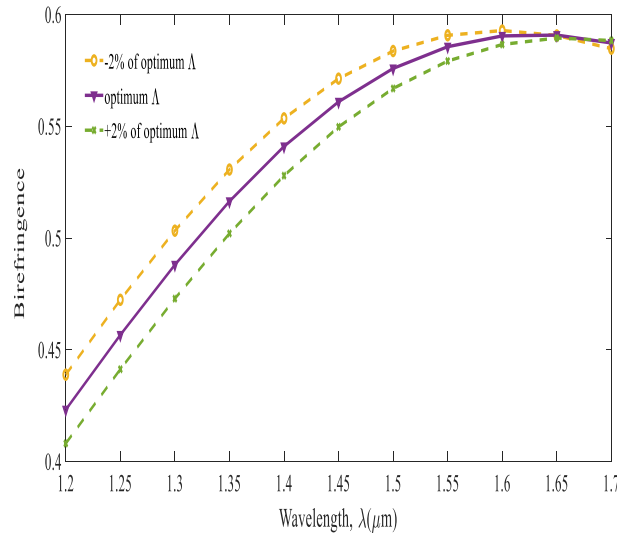


Fig. 3. Birefringence of the modeled PCF concerning the wavelength when the pitch is varied for $\pm 2\%$ of optimum.

Fig. 3 shows the birefringence response with respect to the wavelength. It is apparent from Fig. 3 that the minimum Br is observed at the wavelength of $1.2 \mu\text{m}$ and the wavelength increases with the increment of Br. It is worth noting that the maximum birefringence is observed at the wavelength of $1.55 \mu\text{m}$. As the wavelength increases, the light asymmetry in the core also increases, resulting in a difference between the major and minor axes confinements and consequently, Br increases as well. Further, it is obvious from Fig. 3 that the optimum value of Br slightly increases from 0.58563 to 0.59072 due to a -2% optimum variation in pitch, whereas the optimum Br insignificantly reduces to 0.579202 when an optimum pitch variation of $+2\%$ is performed at the operating wavelength of $1.55 \mu\text{m}$.

Thus, it can be stated from Fig. 3 that not much change is noticeable here as a result of the variation. It is worth mentioning that the ultra-high Br traits are useful in a wide range of applications. It aids in the reduction of the PMD effect, as well as in the prolonged distance communication systems [38, 56], for example. Accordingly, we can conclude that our modeled PCF is capable of playing a critical part in obtaining ultra-high Br.

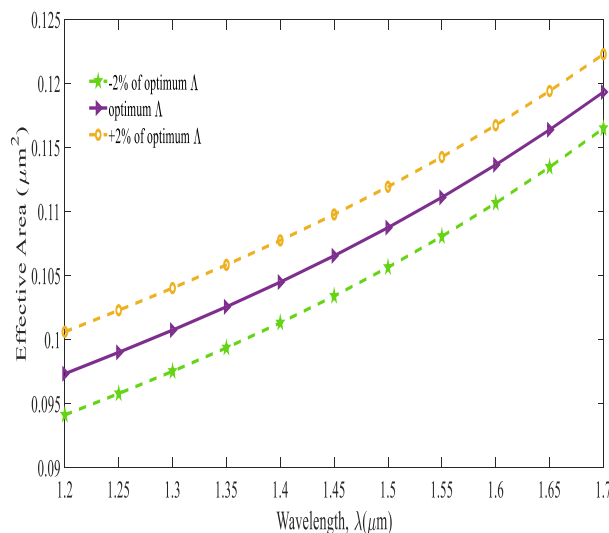


Fig. 4. The response of effective area vs wavelength when the pitch is varied for $\pm 2\%$ of its optimum value.

Fig. 4 presents the behavior of the effective area concerning the wavelength. The wavelength increases with the increment of the effective area, as illustrated in Fig. 4. Increasing the wavelength increases the tendency of the light to move out of the core, which results in the increment of the area light confinement. It is evident from Fig. 4 that $\pm 2\%$ pitch variation results in a very negligible change in our obtained result and for this reason, we hope that our proposed design will perform significantly well even if fabricated.

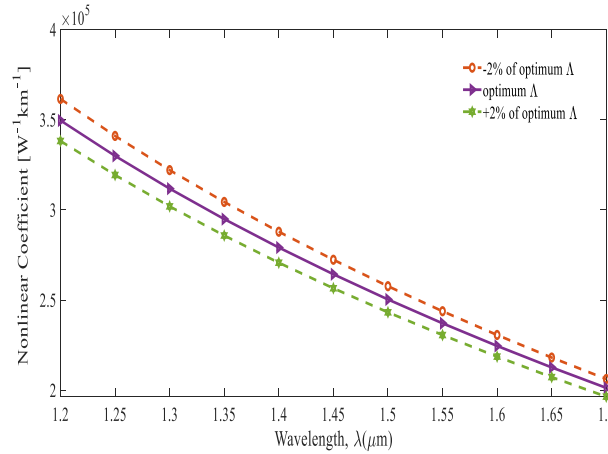


Fig. 5. Nonlinearity vs wavelength when the pitch is varied for $\pm 2\%$ of its optimum value.

Fig. 5 displays the nonlinear characteristics concerning the wavelength. The effective area is inversely proportional to the nonlinearity of the system under consideration, as expressed in equation 4. Besides, the effective area expands as the wavelength increases due to the fact nonlinearity and effective area are inversely related and therefore, the nonlinearity diminishes as the wavelength increases, as demonstrated in Fig. 5. So, taking the curves of Figs. 4 and 5 into consideration, it can be stated the designed PCF performs well theoretically. It is further seen in Fig. 5 that the maximum nonlinearity of $3.49 \times 10^5 W^{-1}Km^{-1}$ is obtained at $1.20 \mu\text{m}$ wavelength, while the minimum nonlinearity of $2.012 \times 10^5 W^{-1}Km^{-1}$ is reached at the wavelength of $1.70 \mu\text{m}$. It is worth noting that a nonlinearity of $2.37 \times 10^5 W^{-1}Km^{-1}$ is also noticed at the operating wavelength of $1.55 \mu\text{m}$. Moreover, at $1.55 \mu\text{m}$ wavelength, the nonlinearity slightly increases to $2.438 \times 10^5 W^{-1}Km^{-1}$ as a result of -2% pitch variation; on the contrary, the nonlinearity lightly lessens to $2.3056 \times 10^5 W^{-1}Km^{-1}$ when the pitch is set at $+2\%$ of its optimum value. From this, we can say that our obtained optimum results do not change much as a result of $\pm 2\%$ variation, which is a great advantageous side of our modeled PCF. In addition to the numerous other utilizations that high nonlinear fibers are capable of serving, supercontinuum generation is among the most essential ones. For fibers with a high degree of nonlinearity, it is feasible to generate large supercontinuum spectra in a relatively small length of fiber [19, 41]. As a result, our designed PCF will be suitable for a wide range of ultra-high nonlinearity purposes.

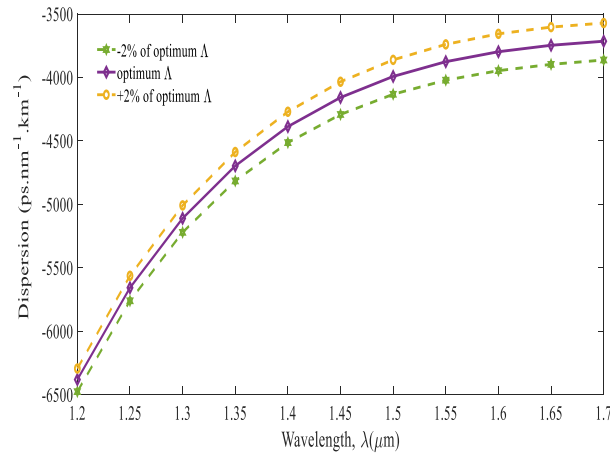


Fig. 6. Dispersion response vs wavelength when the pitch is varied for $\pm 2\%$ of its optimum value.

The dispersion response in terms of wavelength is seen in Fig. 6. The solely independent variable in the modeled design is Λ , all other factors, such as d , m , n and so on, are completely reliant upon it. It is evident from Fig. 6 that the designed PCF always shows negative dispersion between the wavelength ranges of 1.2 to 1.7 μm . The maximum negative dispersion of $-6737.86 \text{ ps.nm}^{-1}.\text{km}^{-1}$ is observed at 1.2 μm wavelength. It is further seen in Fig. 6 that the dispersion curve gradually becomes flattened after the operating wavelength of 1.55 μm and at this wavelength range, a negative dispersion $-3875.21 \text{ ps.nm}^{-1}.\text{km}^{-1}$ is observed.

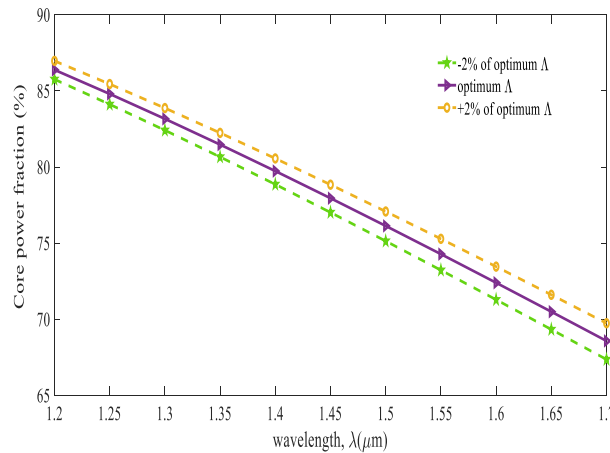


Fig. 7. Power fraction behavior vs wavelength when the pitch is varied for $\pm 2\%$ of its optimum value.

Fig. 7 illustrates the response curve of core power fraction (CPR) with respect to the wavelength. It is apparent from Fig. 7 that as the wavelength increases, the tendency of the light to spread outward from the core increases, resulting in a decrease in CPR. It is worth noting that 86% of the total light confine through the core at 1.2 μm wavelength. However, when the wavelength increases to 1.55 μm , the CPR of the system decreases to 74.28%.

Confinement loss is another leading feature of a PCF. Fig. 8 demonstrates the confinement loss behavior concerning the wavelength. It is obvious from Fig. 8 that increasing the wavelength increases the tendency of the light to move out of the core and as a result, the confinement loss also increases. Here, an optimum pitch variation of $\pm 2\%$ is shown and it is perceived that not much change has been noticed in the result as a result of the variation, which implies that our designed PCF will perform just fine even if fabricated.

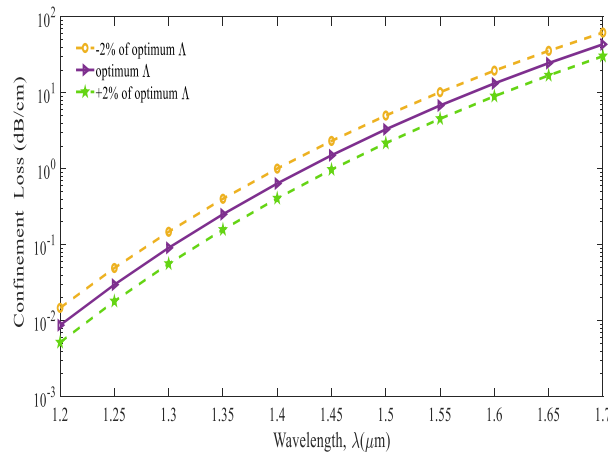


Fig. 8. Confinement loss vs wavelength when the pitch is varied for $\pm 2\%$ of its optimum value.

Table 1. A tabular representation of comparison between our modeled PCF design with other previously published works in the relevant field.

Reference	Birefringence	Nonlinearity $W^{-1}km^{-1}$	Dispersion	Material	Wavelength (μm)
[19]	–	48,850	–	Si ₇ N ₃ , Silica	1
[25]	5.05×10^{-2}	1,896	-500	Tellurite	1.55
[26]	7.57×10^{-2}	188.39	–	Tellurite	1.55
[28]	25.9×10^{-2}	94,700	–	GaP, Silica	1.40
[29]	–	63,435	–	GaP, Silica	1
[30]	25.4×10^{-2}	91,100	-2560.12	As ₂ S ₃ , Silica	–
Proposed	59.1×10^{-2}	237,098	-3875.21	GaP	1.55

From the above table, we can see that the obtained results of our proposed PCF design, such as birefringence, nonlinearity, negative dispersion, etc. are multiple times higher than all other previously reported articles. Nowadays, many researchers are depending on multiple materials to achieve higher optical results. Nevertheless, using two materials simultaneously is troublesome since their melting temperatures will not match, which will make the fabrication process relatively strenuous. However, it is mention-worthy that we have obtained such extremely remarkable outcomes employing a single material (GaP) only so that the fabrication process of our modeled PCF will be comparatively feasible.

5. Fabrication feasibility

One of the most relevant challenges with PCFs lies in fabrication feasibility. Based on our suggested PCF, we can observe in Fig. 1 that it is composed of hexagonally shaped air holes. For this reason, it is fundamental to have fabrication processes that can create a structure with hexagonal geometry to manufacture the PCF that has been presented. Keeping that in mind, there exist a variety of conventional as well as advanced fabrication processes today, including drilling, extrusion and 3D printing, capillary stacking, sol-gel, stack-and-draw, etc. that possess the ability to fabricate a PCF. [52] Among the mentioned fabrication techniques, the stack-and-draw is considered a very popular one. However, such approaches are confined to geometries with the tightest packing like honeycomb or triangular lattices, as well as are not capable of readily constructing circular patterns, as is the case with other methods. Besides, the drilling procedures allow for hole size and spacing adjustments. Nevertheless, they are also most frequently confined

to a modest number of air holes and circular forms. Moreover, the extrusion approaches allow for more design flexibility, although they are ordinarily restrained to soft glasses. A capillary stacking approach was suggested by Argyros et al. [50]. It is possible to efficiently fabricate the suggested PCF employing this approach. Nevertheless, there is a chance that the missing air holes might cause undesired tension during the manufacturing process. So, taking this stress issue caused by a lack of air holes into consideration, we must look for an alternate solution. Conclusively, the sol-gel method was advanced by Bise et al. [51] to create PCFs having any structure, as well as the size and shape of the air holes and the required spacing can all be modified separately. Accordingly, this technique may give necessary extra design freedom for the proposed PCF. Consequently, the stated PCF can be fabricated thanks to the up-to-date advancements in existent fabrication processes.

6. Conclusion

We come up with a unique GaP-based PCF with hexagonal air hole arrangements in this research article that exhibits an ultra-high Br and NLC of 59.1×10^{-2} and $2.37 \times 10^5 \text{ W}^{-1}\text{Km}^{-1}$ sequentially, at the wavelength of $1.55 \mu\text{m}$. Besides, we have precisely adjusted geometric parameters of the GaP-filled PCF by employing the FEM-based COMSOL software. Moreover, we have rigorously assessed several other critical guiding properties concerning the optical wavelength, among which, CL, CPF, effective area, dispersion, etc. are mention-worthy. Conclusively, we believe that our advanced PCF will be an excellent candidate in the diverse fields of optics and photonics, namely supercontinuum generation, telecommunications, biomedical imaging and signal processing, exceptionally high nonlinear utilization and so on.

Acknowledgments

This work was supported by Researchers Supporting Project number (RSP-2021/100), King Saud University, Riyadh, Saudi Arabia. This work was supported in part by funding from the Natural Sciences and Engineering Research Council of Canada (NSERC).

References

- [1] J. C. Knight, T. A. Birks, P. J. St Russell, D. M. Atkin, *Optics Letters*, vol. 21, no. 19, pp. 1547-1549, 1996; <https://doi.org/10.1364/OL.21.001547>.
- [2] F. Luan et al., *Optics Express*, vol. 12, no. 5, pp. 835-840, 2004
<https://doi.org/10.1364/OPEX.12.000835>
- [3] J. C. Knight and P. S. J. Russell, *Science*, vol. 296, no. 5566, pp. 276-277, Apr. 12, 2002;
<https://doi.org/10.1126/science.1070033>
- [4] P. Russell, *Science*, vol. 299, no. 5605, pp. 358-362, Jan. 17, 2003;
<https://doi.org/10.1126/science.1079280>
- [5] P. Russell, *IEEE Leos Newsletter*, vol.21, no. 10, pp. 1–5, 2007.
- [6] H. Talukder, M. I. A. Isti, S. Nuzhat, S. K. Biswas, *Brazilian Journal of Physics*, vol. 50, no. 3, pp. 263-271, Jun. 2020; <https://doi.org/10.1007/s13538-020-00742-1>
- [7] Md. B. Hossain, A. A.-M. Bulbul, Md. A. Mukit, E. Podder, *Optics and Photonics Journal*, vol. 07, no. 11, pp. 235-243, 2017; <https://doi.org/10.4236/opj.2017.711021>
- [8] F. Poli, A. Cucinotta, S. Selleri, *Photonic crystal fibers: properties and applications*, Berlin: Springer, vol. 102, 2007.
- [9] G. K. L. Wong, A. Y. H. Chen, S. W. Ha, R. J. Kruhlak, S. G. Murdoch, R. Leonhardt, J. D. Harvey, N. Y. Joly, *Optics Express*, vol. 13, no. 21, pp. 8662-8670, 2005;
<https://doi.org/10.1364/OPEX.13.008662>

- [10] D. Chen, M. L. V. Tse, H. Y. Tam, Progress In Electromagnetics Research, vol. 105, pp. 193-212, 2010; <https://doi.org/10.2528/PIER10042706>
- [11] S. M. Abdur Razzak, Y. Namihira, F. Begum, S. Kaijage, T. Kinjo, J. Nakahodo, K. Miyagi, N. Zou, Conf. on Optical Fiber Communication and the National Fiber Optic Engineers Conf., pp. 1-6, 2007; <https://doi.org/10.1109/OFC.2007.4348389>
- [12] A. Ortigosa-Blanch et al., Optics Letters, vol. 25, no. 18, pp. 1325-1327, 2000; <https://doi.org/10.1364/OL.25.001325>
- [13] T. P. Hansen et al., IEEE Photonics Technology Letters, vol. 13, no. 6, pp. 588-590, 2001 <https://doi.org/10.1109/68.924030>
- [14] N. G. R. Broderick, T. M. Monroe, P. J. Bennett, D. J. Richardson, Optics Letters, vol. 24, no. 20, pp. 1395-1397, 1999; <https://doi.org/10.1364/OL.24.001395>
- [15] R. K. Sinha, S. K. Varshney, Microwave and Optical Technology Letters, vol. 37, no. 2, pp. 129-132, Apr. 2003; <https://doi.org/10.1002/mop.10845>
- [16] L. Tian, L. Wei, F. Guoying, Optics Communications, vol. 334, pp. 196-202, Jan. 2015; <https://doi.org/10.1016/j.optcom.2014.07.080>
- [17] T. A. Birks, J. C. Knight, P. J. St Russell, Optics Letters, vol. 22, no. 13, pp. 961-963, 1997 <https://doi.org/10.1364/OL.22.000961>
- [18] H. Ademgil, S. Haxha, Sensors (Switzerland), vol. 15, no. 12, pp. 31833-31842, Dec. 2015 <https://doi.org/10.3390/s151229891>
- [19] B. K. Paul, K. Ahmed, Ceramics International, vol. 45, no. 1, pp. 1215-1218, Jan. 2019 <https://doi.org/10.1016/j.ceramint.2018.09.307>
- [20] T. Yang, E. Wang, H. Jiang, Z. Hu, K. Xie, Optics Express, vol. 23, no. 7, p. 8329, Apr. 2015; <https://doi.org/10.1364/OE.23.008329>
- [21] B. Yu, H. Rui, Optical and Quantum Electronics, vol. 51, no. 11, Nov. 2019 <https://doi.org/10.1007/s11082-019-2091-6>
- [22] S. Hossain, S. Shah, M. Faisal, Optik, vol. 225, Jan. 2021; <https://doi.org/10.1016/j.ijleo.2020.165753>
- [23] Z. Hui, Y. Zhang, A. H. Soliman, Ceramics International, vol. 44, no. 9, pp. 10383-10392, Jun. 2018; <https://doi.org/10.1016/j.ceramint.2018.03.052>
- [24] H. Zhanqiang, Y. Zhang, H. Zhou, Z. Wang, X. Zeng, Fiber and Integrated Optics, vol. 37, no. 1, pp. 21-36, Jan. 2018; <https://doi.org/10.1080/01468030.2017.1423134>
- [25] J. Wang, Applied Optics, vol. 60, no. 15, p. 4455, May 2021; <https://doi.org/10.1364/AO.423029>
- [26] M. Liu, H. Yuan, P. Shum, C. Shao, H. Han, L. Chu, Applied Optics, vol. 57, no. 22, p. 6383, Aug. 2018; <https://doi.org/10.1364/AO.57.006383>
- [27] K. Ahmed, B. K. Paul, M. A. Jabin, B. Biswas, Ceramics International, vol. 45, no. 12, pp. 15343-15347, Aug. 2019; <https://doi.org/10.1016/j.ceramint.2019.05.027>
- [28] M. T. Anas, S. Asaduzzaman, K. Ahmed, T. Bhuiyan, Results in Physics, vol. 11, pp. 1039-1043, Dec. 2018; <https://doi.org/10.1016/j.rinp.2018.11.013>
- [29] B. K. Paul, M. Golam Moctader, K. Ahmed, M. Abdul Khalek, Results in Physics, vol. 10, pp. 374-378, Sep. 2018; <https://doi.org/10.1016/j.rinp.2018.06.033>
- [30] M. M. Hassan, K. Ahmed, B. K. Paul, M. N. Hossain, F. A. al Zahrani, Physica Scripta, vol. 96, no. 11, Nov. 2021; <https://doi.org/10.1088/1402-4896/ac13e1>
- [31] K. Ahmed et al., Materials Discovery, vol. 7, pp. 8-14, Mar. 2017; <https://doi.org/10.1016/j.md.2017.05.002>
- [32] K. Ahmed et al., Alexandria Engineering Journal, vol. 57, no. 4, pp. 3683-3691, Dec. 2018; <https://doi.org/10.1016/j.aej.2018.01.018>
- [33] P. A. Agbemabiese, E. K. Akowuah, Journal of Optical Communications, 2020; <https://doi.org/10.1515/joc-2020-0084>
- [34] S. Abedin, A. Hira, S. Mohammad Tadvin, Journal of Advanced Optics and Photonics, vol. 1, no. 3, pp. 235-249, 2018; <https://doi.org/10.32604/jaop.2018.03869>
- [35] A. Upadhyay, S. Singh, D. Sharma, S. A. Taya, 2021; <https://doi.org/10.21203/rs.3.rs-227813/v1>

- [36] T. Zhao, Z. Lian, T. Benson, X. Wang, W. Zhang, S. Lou, *Optical Materials*, vol. 73, pp. 343-349, Nov. 2017; <https://doi.org/10.1016/j.optmat.2017.07.010>
- [37] F. Li et al., *Optical Materials*, vol. 79, pp. 137-146, May 2018; <https://doi.org/10.1016/j.optmat.2018.03.025>
- [38] R. Amin, M. Enam Khan, F. Ahmed Al-Zahrani, K. Ahmed, *Physica Scripta*, August 2021; <https://doi.org/10.1088/1402-4896/ac227c>
- [39] Fiore Andrea et al., *J. Nonlinear Opt. Phys. Mater.*, vol. 05, no. 04, pp. 645-651, 1996 <https://doi.org/10.1142/S0218863596000477>
- [40] T. Skauli et al., *Journal of Applied Physics*, vol. 94, no. 10, pp. 6447-6455, Nov. 2003 <https://doi.org/10.1063/1.1621740>
- [41] R. Amin, L. F. Abdulrazak, N. Mohammadd, K. Ahmed, F. M. Bui, S. M. Ibrahim, *Ceramics International*, Nov. 2021; <https://doi.org/10.1016/j.ceramint.2021.11.106>
- [42] P. J. Dean, G. Kaminsky, R. B. Zetterstrom, *Journal of Applied Physics*, vol. 38, no. 9, pp. 3551-3556, 1967; <https://doi.org/10.1063/1.1710170>
- [43] D. F. Parsons, P. D. Coleman, *Applied Optics*, vol. 10, no. 7, pp. 1683-1685, 1971; https://doi.org/10.1364/AO.10.1683_1
- [44] J. Wei, J. M. Murray, J. O. Barnes, D. M. Krein, P. G. Schunemann, S. Guha, *Optical Materials Express*, vol. 8, no. 2, p. 485, Feb. 2018; <https://doi.org/10.1364/OME.8.000485>
- [45] B. K. Paul et al., *Alexandria Engineering Journal*, vol. 59, no. 6, pp. 5045-5052, Dec. 2020 <https://doi.org/10.1016/j.aej.2020.09.030>
- [46] B. K. Paul, K. Ahmed, M. Thillai Rani, K. P. Sai Pradeep, F. A. Al-Zahrani, *Alexandria Engineering Journal*, 2021; <https://doi.org/10.1016/j.aej.2021.08.006>
- [47] F. Liu et al., *Journal of Optics*, vol. 12, no. 9, 2010; <https://doi.org/10.1088/2040-8978/12/9/095201>
- [48] S. Matloub, R. Ejlali, A. Rostami, *Progress In Electromagnetics Research C*, vol. 60, pp. 115-123, 2015; <https://doi.org/10.2528/PIERC15091901>
- [49] M. R. Hasan et al., *IEEE Sensors Journal*, vol. 18, no. 1, pp. 133-140, Jan. 2018; <https://doi.org/10.1109/JSEN.2017.2769720>
- [50] A. Argyros et al., *Optics Express*, vol. 9, no. 13, pp. 813-820, 2001; <https://doi.org/10.1364/OE.9.000813>
- [51] R. T. Bise, D. J. Trevor, *OFC/NFOEC Technical Digest. Optical Fiber Communication Conference*, 2005; <https://doi.org/10.1109/OFC.2005.192772>
- [52] M. I. Hasan, M. Selim Habib, M. Samiul Habib, S. M. Abdur Razzak, *Optical Fiber Technology*, vol. 20, no. 1, pp. 32-38, 2014; <https://doi.org/10.1016/j.yofte.2013.11.005>
- [53] S. R. Tahhan, A. J. Ghazai, I. M. Alwan, M. H. Ali, *Digest Journal of Nanomaterials and Biostructures*, vol. 14, no. 3, pp. 831 – 841, 2019.
- [54] S. R. Tahhan, H. K. Aljobouri, *Journal of Optical Communications*, 2020; <https://doi.org/10.1515/joc-2019-0291>
- [55] S. R. Tahhan, M. H. Ali, M. A. Z. Al-Ogaidi, A. K. Abass, *Journal of Communications*, vol. 14, no. 1, pp. 53-57, Jan. 2019; <https://doi.org/10.12720/jcm.14.1.53-57>
- [56] R. Amin et al., *Physica Scripta*, 2022; <https://doi.org/10.1088/1402-4896/ac5359>